

# **Two new three-dimensional contact algorithms for staggered Lagrangian Hydrodynamics**

**Zupeng Jia**

**Institute of Applied Physics and Computational  
Mathematics, Beijing 100094, China**

**2023.5.2**





ELSEVIER

Contents lists available at [ScienceDirect](#)

## Journal of Computational Physics

[www.elsevier.com/locate/jcp](http://www.elsevier.com/locate/jcp)

### Two new three-dimensional contact algorithms for staggered Lagrangian Hydrodynamics

Zupeng Jia<sup>a,\*</sup>, Xiangfei Gong<sup>a</sup>, Shudao Zhang<sup>a,b</sup>, Jun Liu<sup>a</sup>

<sup>a</sup> Institute of Applied Physics and Computational Mathematics, Beijing 100094, China

<sup>b</sup> Center of Applied Physics and Technology, Peking university, Beijing 100871, China

# Outline

- **Review on contact search algorithms**
- **Review on contact enforcement algorithms**
- **Method 1: discrete accurate matching method**
- **Method 2: discrete Lagrangian multiplier method**
- **Parallel implementation**
- **Numerical results**
- **Conclusion**



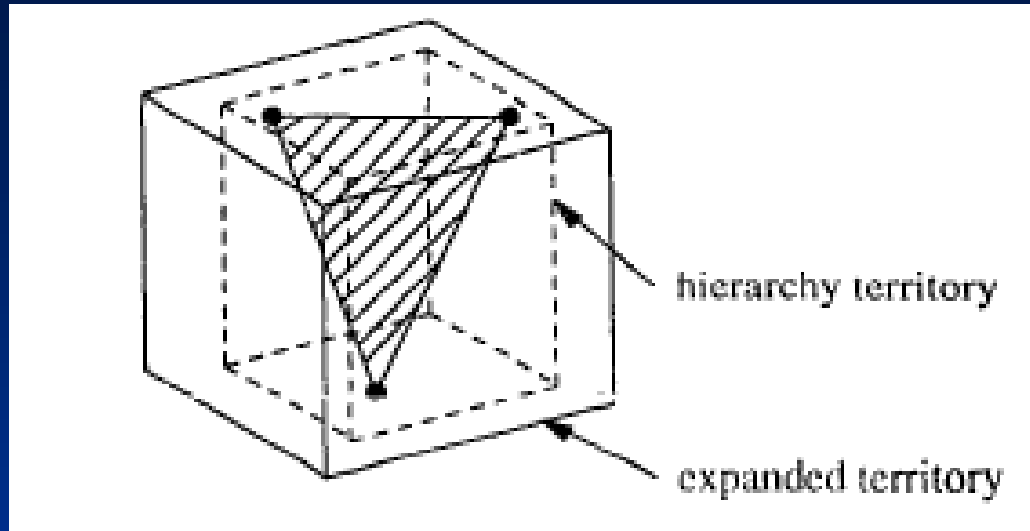
# 1. Review on contact search algorithms

- Contact search is used to detect where contact occurs.
- Contact search generally involves a global search followed by a local search.
- The global search roughly determines the nodes that may come into contact with a segment / edge / node, that is, to identify all test pairs.
- The local search accurately calculates the position of a contact node in relation to its target segment / edge / node .



- **Global search algorithms may be categorized into**
  - ✓ **The bucket sorting algorithm**  
(Belytschko, 1987; Benson, 1990; Hallquist 2005)
  - ✓ **The spherical sorting algorithm**  
(Papadopoulos, 1993)
  - ✓ **The linear position code algorithm (Oldenburg, 1994)**
  - ✓ **The hierarchy-territory algorithm (Zhong, 1996)**
  - ✓ **The unified algorithm. (Zhong, 1996)**  
In the unified algorithm, segments from all contact surfaces are treated as a single set, and the hierarchy territory and bucket sort algorithm are used to find out test pairs efficiently.





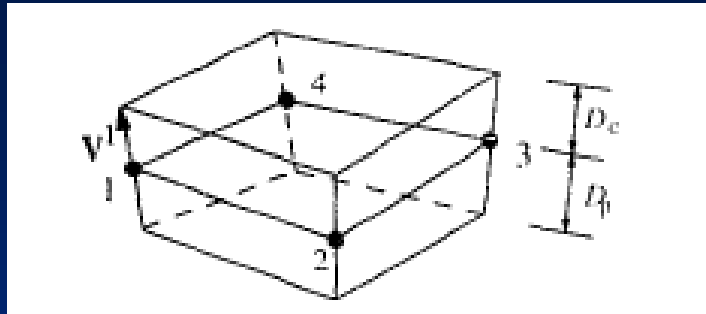
**Expanded territory of a triangle segment  
(the brick made up of solid lines)**

**If a node falls into this expanded territory, then this node and the segment may come into contact, forming a test pair.**

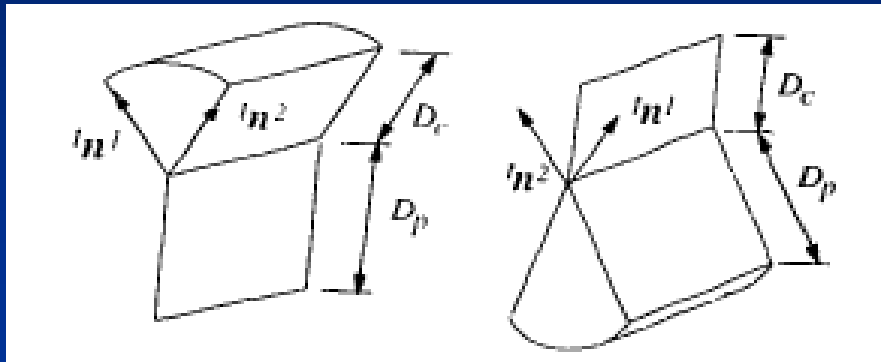
- **Local search algorithms may be categorized into**
  - ✓ **Node-to-segment algorithm (Hallquist 1985)**
  - ✓ **Pinball algorithm (Belytschko, 1989)**
  - ✓ **Inside-outside algorithm (Wang, 1997)**
  - ✓ **Free-formed-surface (FFS) algorithm(Wang, 2001)**
  - ✓ **Splitting pinball algorithm (Belytschko, 1993)**

**Local search accurately locates the target point of a node, calculates the penetration of the target point relative to it, and judges the contact status of the target point, in order to find all contact pairs from the test pairs.**

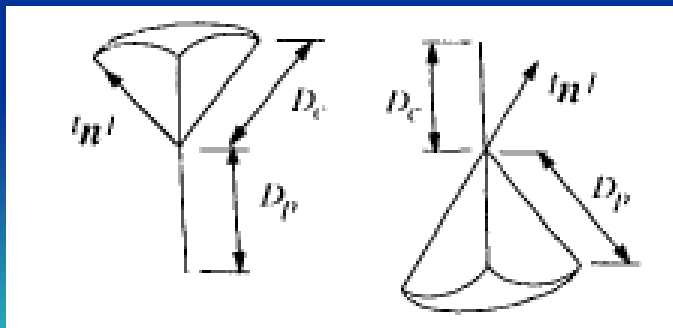




**Contact territory of a segment / edge / node**



**If a node falls into the contact territory of a segment / edge / point, the two come into contact and form a contact pair.**





**Considering the computational workload, programming workload, user convenience, and applicability, for the global search we adopt the unified algorithm, while for the local search we adopt the node-to-segment algorithm.**



## 2. Review on contact enforcement algorithms

- Once the contact search is completed and the depths of penetrations are computed, the next step is to remove the penetrations by applying appropriate forces. The process is known as contact enforcement.
- Contact enforcement algorithms can be mainly classified into three groups:
  - ✓ The distributed parameter method
  - ✓ The Lagrangian multiplier method
  - ✓ The penalty method

Each with advantages and disadvantages.

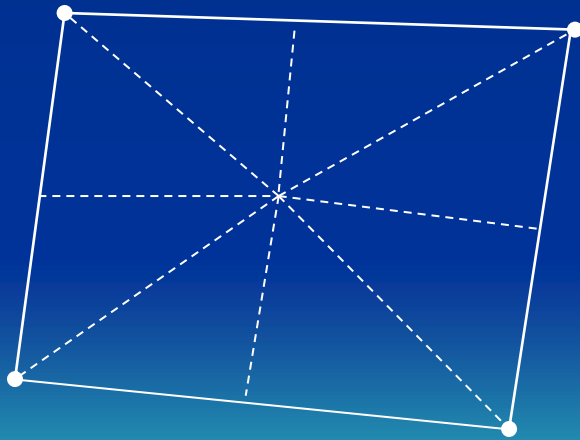


### 3. Method 1: discrete accurate matching method

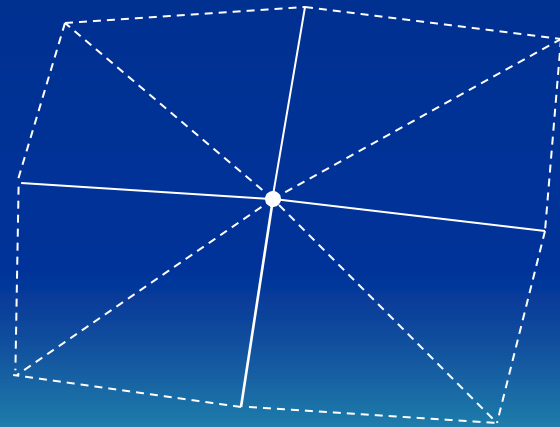
- This method is used for master–slave type of contact.
- **Step 1** Calculate the nodal mass  $m_s(n)$  and nodal forces  $f_{x1}(n)$ ,  $f_{x2}(n)$ ,  $f_{x3}(n)$  of every contact node  $n$  using free surface boundary conditions.
- **Step 2** Partition each contact segment into triangular facets using the nodes that make up the segment, the center of it and the midpoints of its edges.



- For a quadrilateral segment, this is illustrated in the following figure (left). Correspondingly, each contact node is surrounded by several such triangular facets, see figure (right).
- Define the nodal area  $sp(n)$  to be the sum of the areas of these triangular facets that surround each node  $n$ .

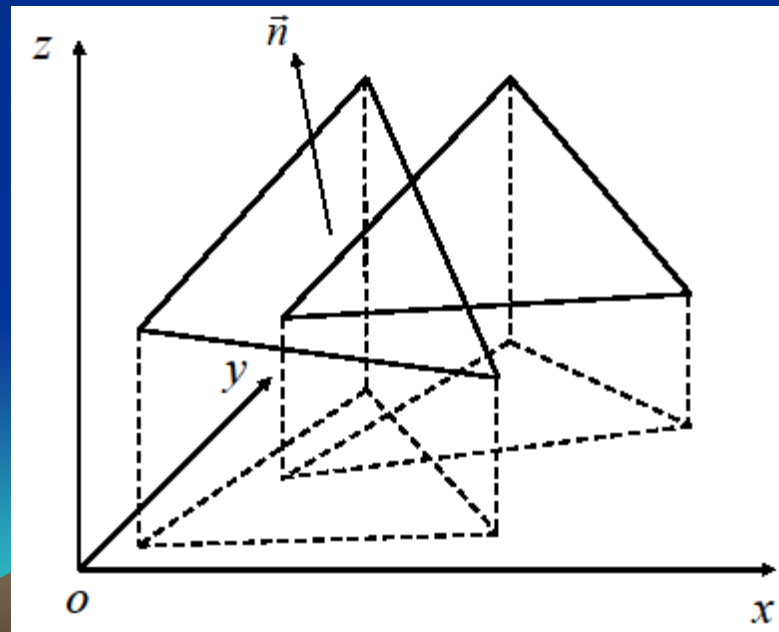


Segment divided into facets



Facets surround a node

- **Step 3** Consider a contact pair, such as a node-to-segment pair. For each facet that surrounds the node and each facet of the segment, by projecting the vertexes of these two facets to the plane in which the former facet lies, two triangles are obtained. Then calculate the intersection area  $s_0$  of these two triangles.



- **Suppose that the facet of the segment corresponds to the node  $m$ . The nodal mass, nodal forces and nodal area of it are respectively**

$$ms(m) \quad fx1(m), fx2(m), fx3(m) \quad sp(m)$$

- **Then the mass and forces carried by the intersection portion of the facet which corresponds to the node  $n$  and node  $m$  are calculated respectively as**

$$ms(n) \frac{s0}{sp(n)} \quad fx1(n) \frac{s0}{sp(n)}, fx2(n) \frac{s0}{sp(n)}, fx3(n) \frac{s0}{sp(n)}$$

$$ms(m) \frac{s0}{sp(m)} \quad fx1(m) \frac{s0}{sp(m)}, fx2(m) \frac{s0}{sp(m)}, fx3(m) \frac{s0}{sp(m)}$$

- **Step 4** Add the mass and forces carried by the intersection portion of each facet to the corresponding node of the opposite triangular facet.

$$\overline{ms}(n) = \overline{ms}(n) + ms(m) \frac{s_0}{sp(m)} \quad \overline{ms}(m) = \overline{ms}(m) + ms(n) \frac{s_0}{sp(n)}$$

$$\overline{fx1}(n) = \overline{fx1}(n) + fx1(m) \frac{s_0}{sp(m)}, \quad \overline{fx1}(m) = \overline{fx1}(m) + fx1(n) \frac{s_0}{sp(n)},$$

$$\overline{fx2}(n) = \overline{fx2}(n) + fx2(m) \frac{s_0}{sp(m)}, \quad \overline{fx2}(m) = \overline{fx2}(m) + fx2(n) \frac{s_0}{sp(n)},$$

$$\overline{fx3}(n) = \overline{fx3}(n) + fx3(m) \frac{s_0}{sp(m)} \quad \overline{fx3}(m) = \overline{fx3}(m) + fx3(n) \frac{s_0}{sp(n)}$$



- For other kinds of contact pairs, such as node-to-edge contact pairs and node-to-node contact pairs, similar procedures can be done.
- **Step 5** Update the accelerations of the contact nodes

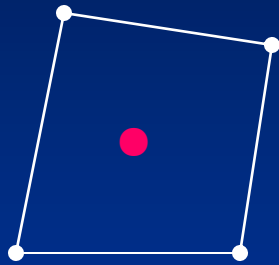
$$a_1(n) = \frac{\overline{fx1}(n)}{\overline{ms}(n)} \quad , \quad a_2(n) = \frac{\overline{fx2}(n)}{\overline{ms}(n)} \quad , \quad a_3(n) = \frac{\overline{fx3}(n)}{\overline{ms}(n)}$$

- **Step 6** Adjust the normal components of the accelerations and velocities of the slave nodes. This step is the “put-back-on” step and is done only for master–slave type of contact.

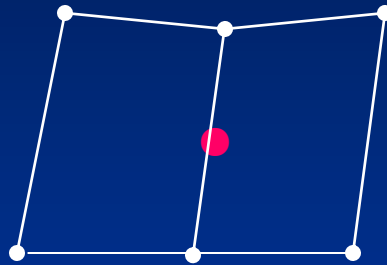




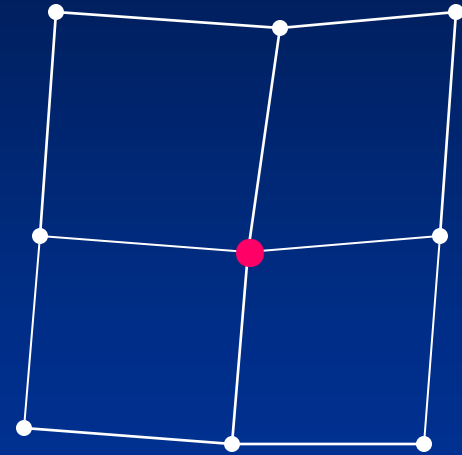
- **First, for each slave node, select at least four master nodes that are nearest to the slave node.**



**Node-to-segment**



**Node-to-edge**



**Node-to-node**

- **Next, calculate the normal components of the accelerations and velocities of the selected master nodes.**

- **Then the normal components of the accelerations and velocities of the slave node are calculated by radial basis function interpolation method using the coordinates and the normal components of the accelerations and velocities of the selected master nodes.**
- **The tangential components of the accelerations and velocities of all slave nodes remain unchanged.**
- **Theoretically, the discrete accurate matching method guarantees zero penetration and conservation of momentum. But in practical simulation this cannot be guaranteed due to numerical errors.**

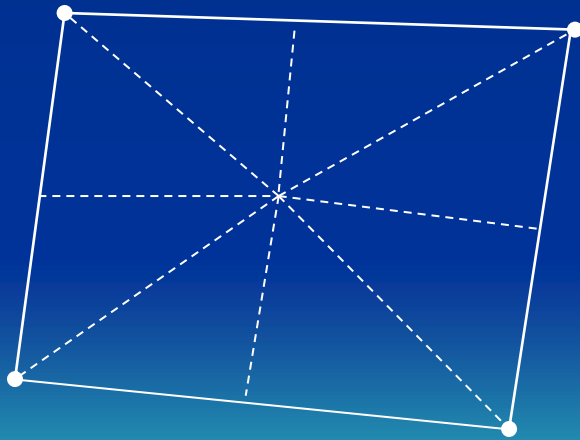


## 4. Method 2: discrete Lagrangian multiplier method

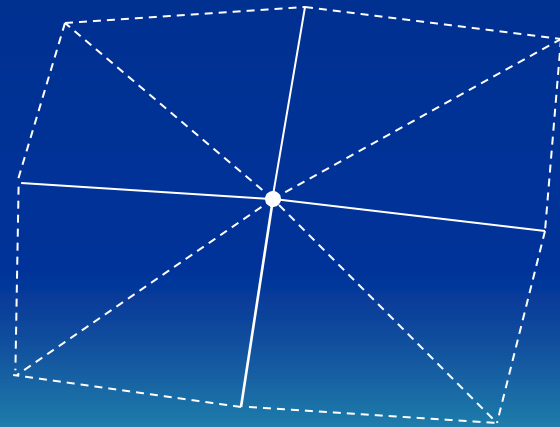
- **Step 1** Calculate the nodal mass  $m_s(n)$  and nodal forces  $f_{x1}(n), f_{x2}(n), f_{x3}(n)$  of every contact node  $n$  using free surface boundary conditions.
- **Step 2** Partition the segment into triangular facets using the nodes that make up the segment, the center of it and the midpoints of its edges.



- For a quadrilateral segment, this is illustrated in the following figure (left). Correspondingly, each contact node is surrounded by several such triangular facets, see figure (right).
- Define the nodal area  $sp(n)$  to be the sum of the areas of these triangular facets that surround each node  $n$ .

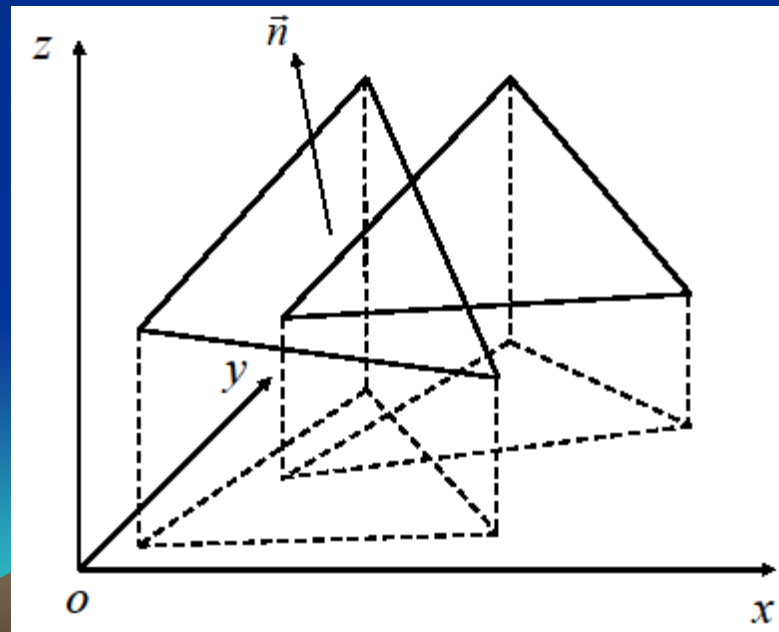


Segment divided into facets



Facets surround a node

- **Step 3** Consider a contact pair, such as a node-to-segment pair. For each facet that surrounds the node and each facet of the segment, by projecting the vertexes of these two facets to the plane in which the former facet lies, two triangles are obtained. Then calculate the intersection area  $s_0$  of these two triangles.



- **Suppose that the facet of the segment corresponds to the node  $m$ . The nodal mass, nodal forces and nodal area of it are respectively**

$$ms(m) \quad fx1(m), fx2(m), fx3(m) \quad sp(m)$$

- **Then the mass and forces carried by the intersection portion of the facet which corresponds to the node  $n$  and node  $m$  are calculated respectively as**

$$ms(n) \frac{s0}{sp(n)} \quad fx1(n) \frac{s0}{sp(n)}, fx2(n) \frac{s0}{sp(n)}, fx3(n) \frac{s0}{sp(n)}$$

$$ms(m) \frac{s0}{sp(m)} \quad fx1(m) \frac{s0}{sp(m)}, fx2(m) \frac{s0}{sp(m)}, fx3(m) \frac{s0}{sp(m)}$$

- **View the intersection portions of the facets which correspond to the hitting node  $n$  and the target node  $m$  as the hitting point and the target point of a 1D contact pair in the normal direction  $(n_x, n_y, n_z)$ , respectively.**
- **Calculate the contact force  $f_h$  for the hitting point of this contact pair using the Lagrangian multiplier method which will be shown in the following.**



- Then add the components in three directions  $x$ ,  $y$ ,  $z$  of the contact force  $f_h$  to the corresponding components of the contact forces of the hitting node  $n$  and the target node  $m$ , respectively.

$$fc1(n) = fc1(n) + f_h \cdot n_x$$

$$fc2(n) = fc2(n) + f_h \cdot n_y$$

$$fc3(n) = fc3(n) + f_h \cdot n_z$$

$$fc1(m) = fc1(m) - f_h \cdot n_x$$

$$fc2(m) = fc2(m) - f_h \cdot n_y$$

$$fc3(m) = fc3(m) - f_h \cdot n_z$$



- For other kinds of contact pairs, such as node-to-edge contact pairs and node-to-node contact pairs, similar procedures can be done.
- **Step 5** Update the accelerations of the contact nodes

$$a_1(n) = (F_1(n) + fc1(n)) / ms(n)$$

$$a_2(n) = (F_2(n) + fc2(n)) / ms(n)$$

$$a_3(n) = (F_3(n) + fc3(n)) / ms(n)$$

- **Step 6** Update the velocities of the contact nodes.



- **It must be noted that, for the discrete Lagrangian multiplier method, a master/slave distinction can not be made and a “put-back-on” step is not needed.**
- **Theoretically, the discrete Lagrangian multiplier method guarantees zero penetration and conservation of momentum. But in practical simulation this cannot be guaranteed due to numerical errors.**



# Calculation of the contact force for contact pair of one hitting node and one target node in 1D

The equations of motion are

$$M_\alpha a_\alpha = F_\alpha + f_\alpha, \quad \alpha = h, d \quad (14)$$

where  $M_\alpha, a_\alpha, F_\alpha, f_\alpha$  are the mass, the acceleration, the nodal force and the contact force of node  $\alpha$ , respectively;  $\alpha = h$  for the hitting node, and  $\alpha = d$  for the target node.

The velocities of the nodes are updated by

$$v_\alpha^{n+1} = v_\alpha^n + \Delta t a_\alpha, \quad \alpha = h, d \quad (15)$$

where  $v_\alpha^n, v_\alpha^{n+1}$  are the velocities at time  $t = t^n$  and time  $t = t^{n+1}$  of node  $\alpha$ , respectively.

The coordinates of the nodes are updated by

$$x_\alpha^{n+1} = x_\alpha^n + \Delta t \frac{v_\alpha^n + v_\alpha^{n+1}}{2} \quad (16)$$

From (14) and (15) we have

$$\begin{aligned} x_\alpha^{n+1} &= x_\alpha^n + \Delta t v_\alpha^n + \frac{1}{2} (\Delta t)^2 a_\alpha \\ &= x_\alpha^n + \Delta t v_\alpha^n + \frac{1}{2} (\Delta t)^2 \frac{F_\alpha + f_\alpha}{M_\alpha} \end{aligned} \quad (17)$$

On the other hand, the zero penetration condition gives that

$$g^{n+1} = g^n + (x_h^{n+1} - x_h^n) - (x_d^{n+1} - x_d^n) = 0 \quad (18)$$

where  $g^n, g^{n+1}$  are the penetrations at time  $t = t^n$  and time  $t = t^{n+1}$ , respectively.

From (17) and (18) we have

$$\begin{aligned} g^n &= (x_d^{n+1} - x_d^n) - (x_h^{n+1} - x_h^n) \\ &= \Delta t v_d^n + \frac{1}{2}(\Delta t)^2 \frac{F_d + f_d}{M_d} - \Delta t v_h^n - \frac{1}{2}(\Delta t)^2 \frac{F_h + f_h}{M_h} \end{aligned} \quad (19)$$

Now, from (19) and  $f_h = -f_d$  we get

$$f_h = \frac{M_h M_d}{M_h + M_d} \left\{ \frac{F_d}{M_d} - \frac{F_h}{M_h} + \frac{v_d^n - v_h^n}{\frac{1}{2}\Delta t} - \frac{g^n}{\frac{1}{2}(\Delta t)^2} \right\} \quad (20)$$

In (18) the zero penetration condition for coordinates is used. We note that the zero penetration condition for velocities can also be used and similar formulae for calculating the contact force can be derived.

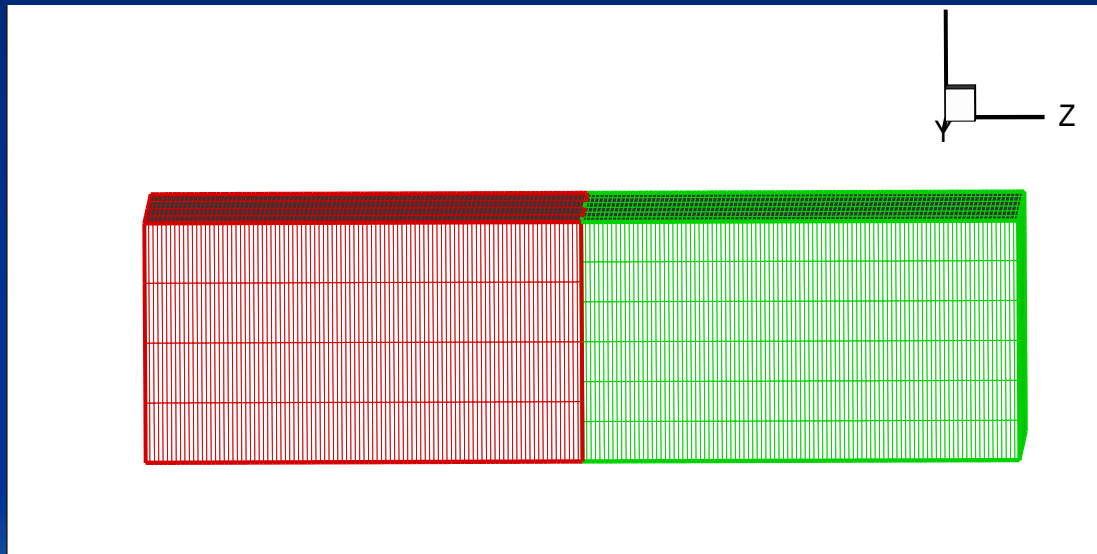
## 5. Parallel implementation

- The software METIS is used to partition the 3D unstructured mesh.
- Unlike the mesh connectivity which does not change during computations, the contact surfaces move relatively.
- In order to maintain dynamic load balancing, we use the recursive coordinate bisection (RCB) algorithm to parallelize the contact algorithms.

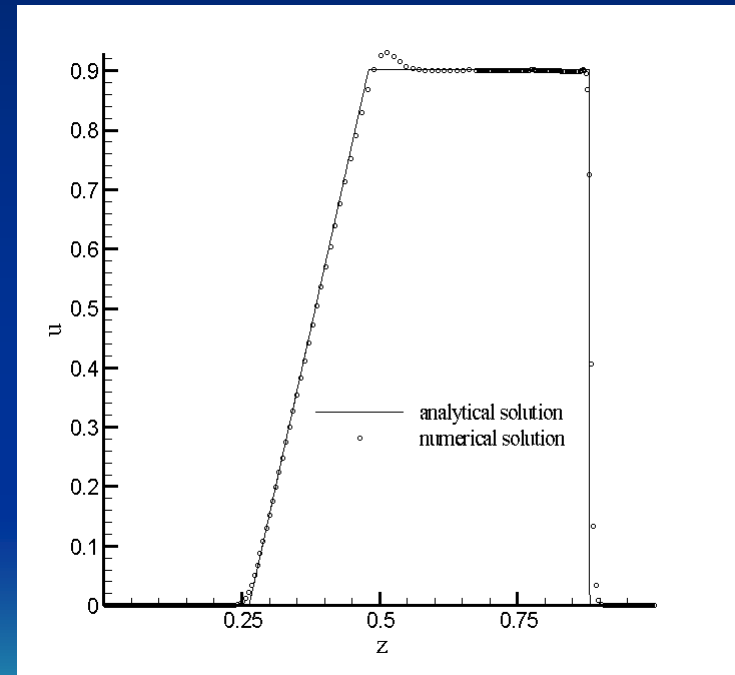
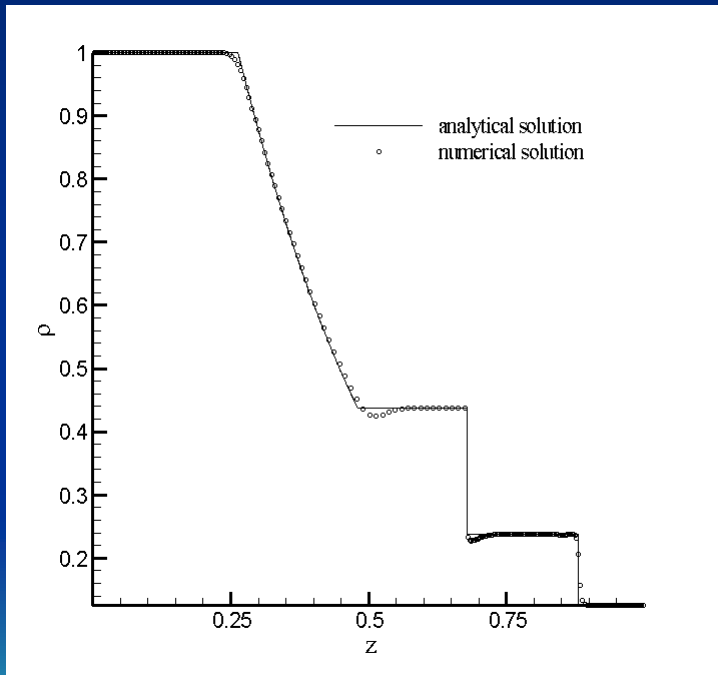
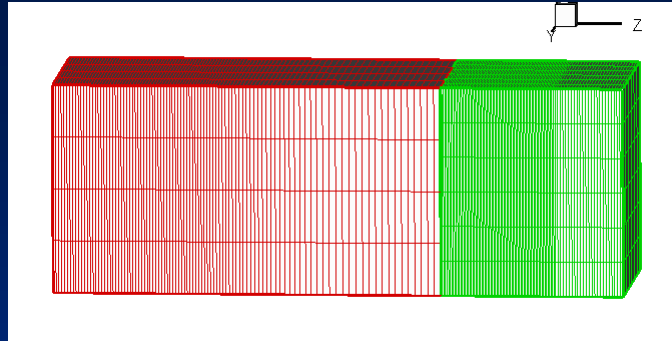


## 6. Numerical results

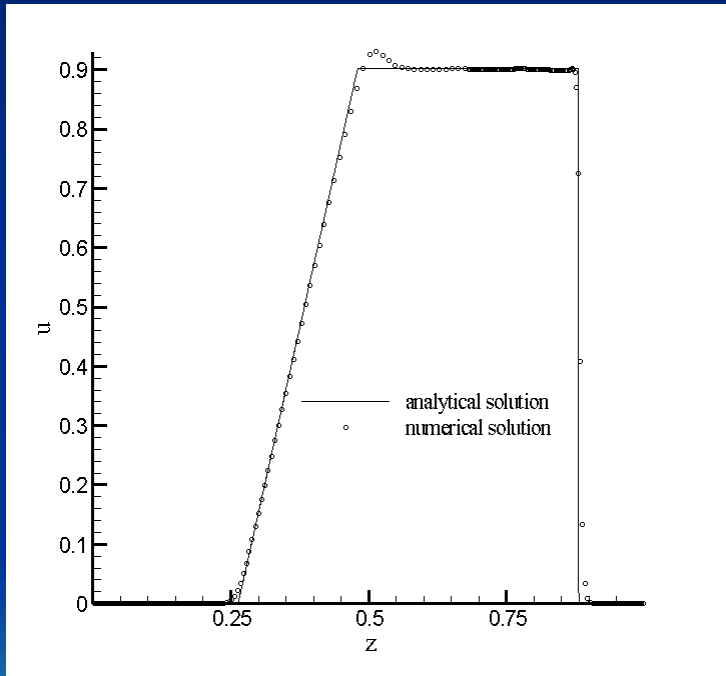
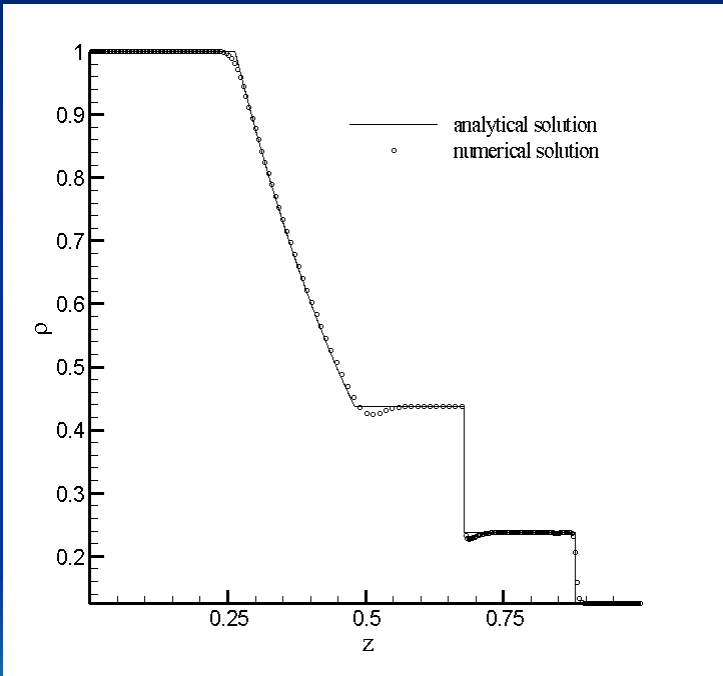
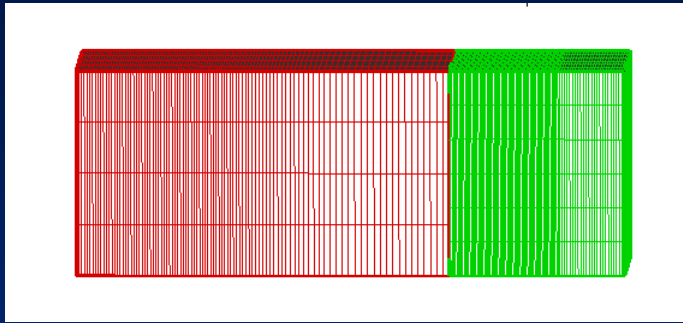
- **Test 1** 1D two-material Sod's shock tube problem



Initial meshes are not matched.



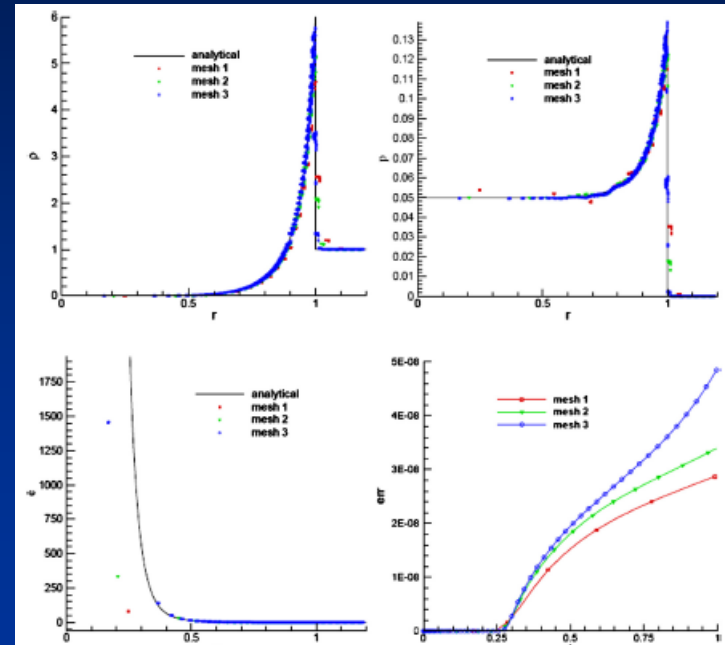
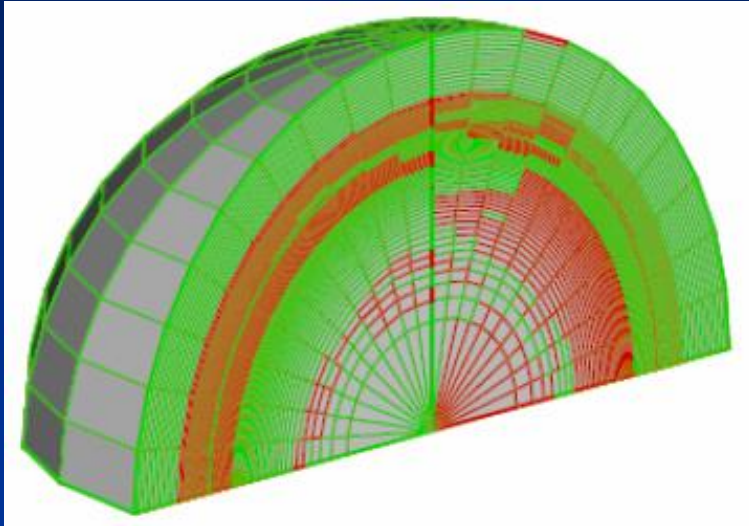
Results of the discrete accurate matching method  
(The DAM method)



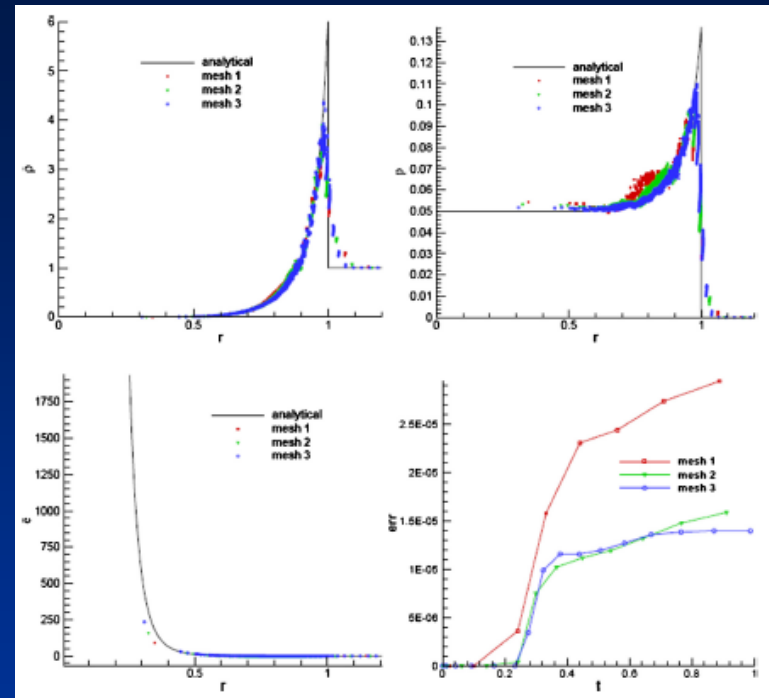
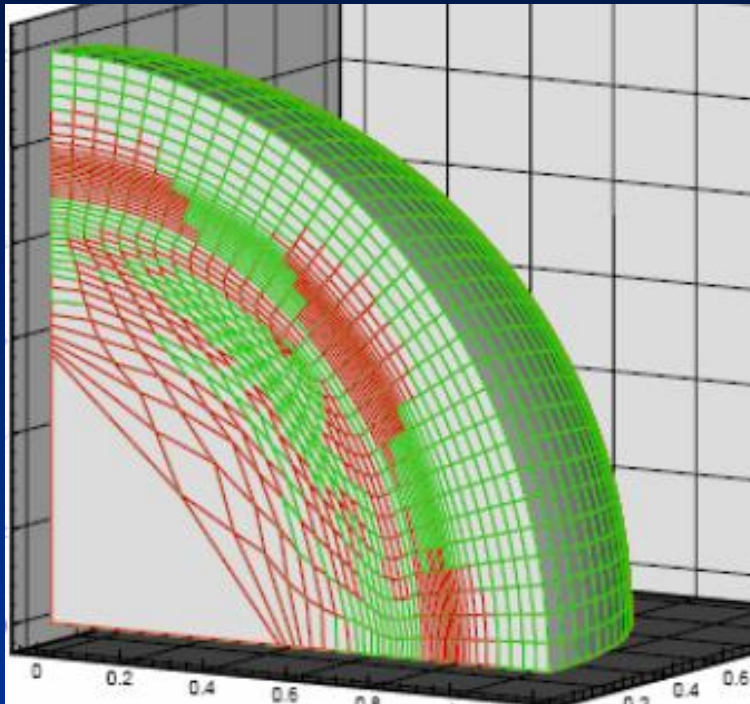
Results of the discrete Lagrangian multiplier method  
(The DLM method)



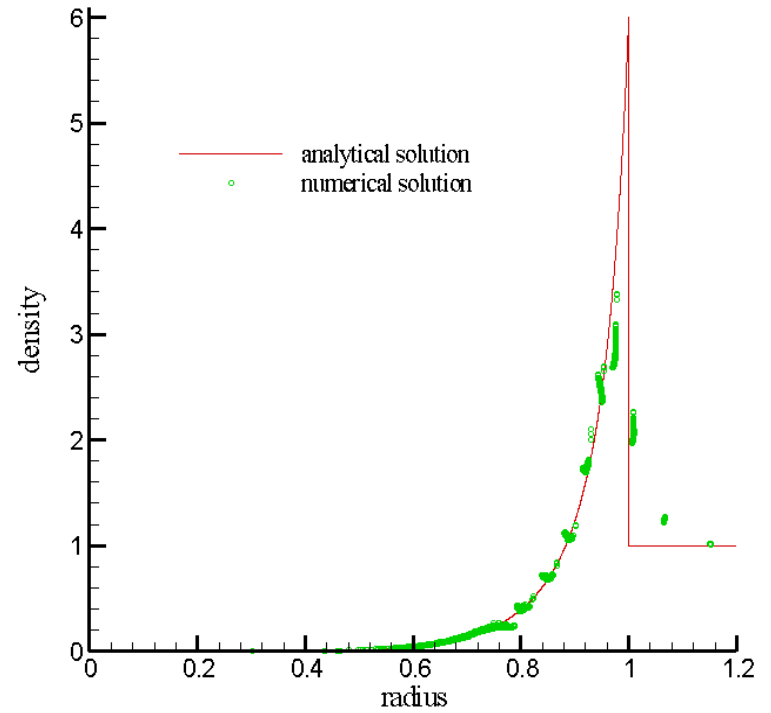
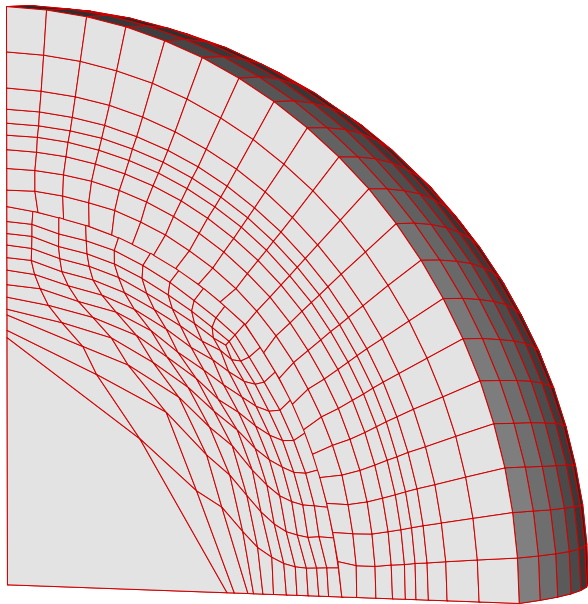
- **Test 2** 3D Sedov problem



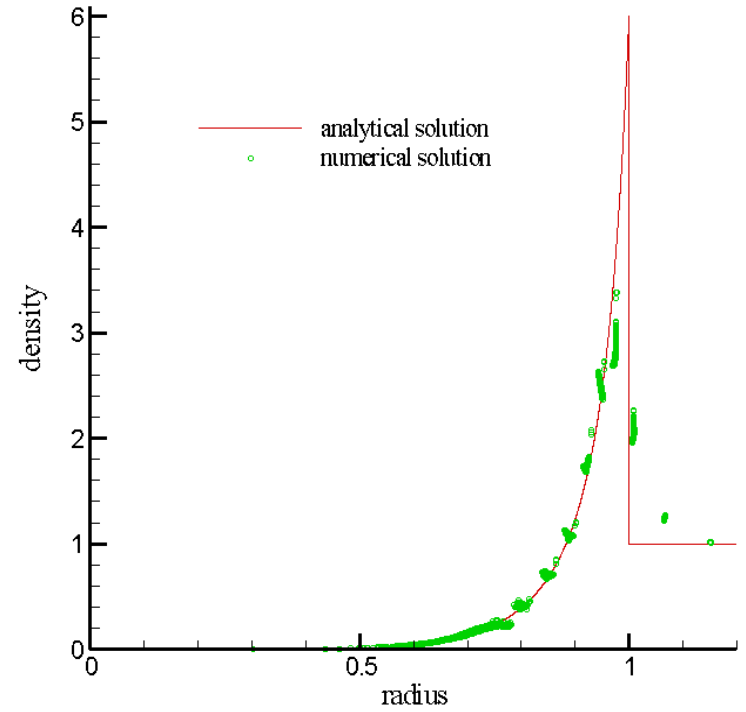
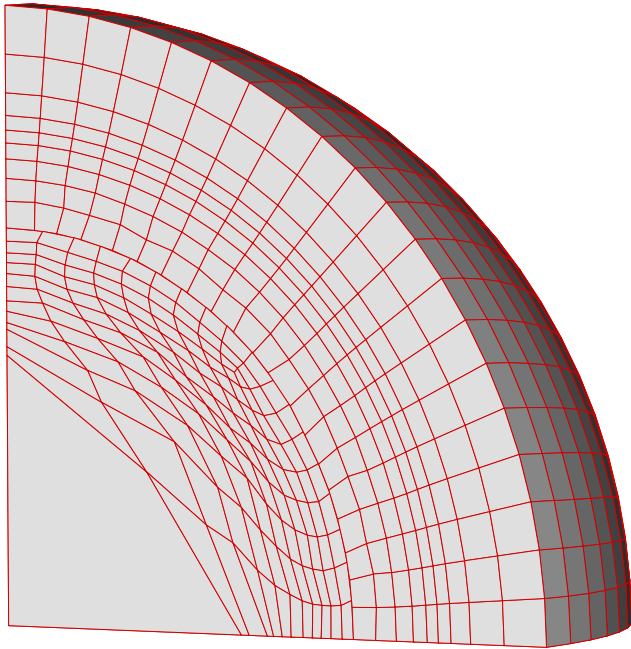
The density (top-left), pressure (top-right), internal energy (bottom-left) at centroids of cells versus the distance of the centroids to the origin at  $t=1$  obtained by the DAM method on three meshes. The relative error of total energy as a function of time (bottom-right) obtained by the DAM method on three meshes.



The density (top-left), pressure (top-right), internal energy (bottom-left) at centroids of cells versus the distance of the centroids to the origin at  $t=1$  obtained by the DLM method on three meshes. The relative error of total energy as a function of time (bottom-right) obtained by the DLM method on three meshes.

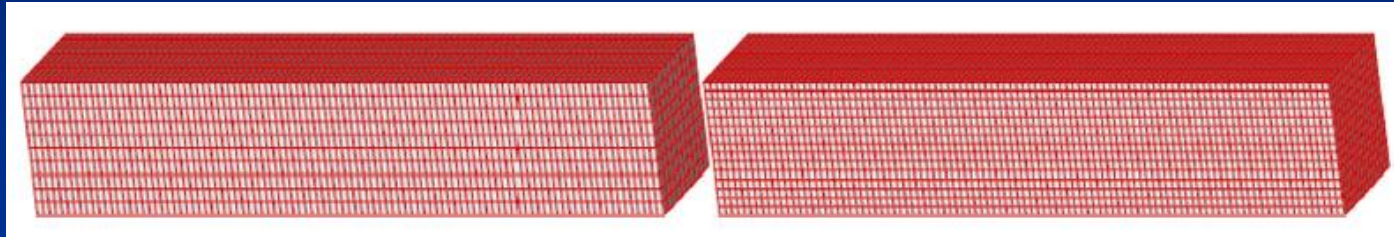


## Results of the DAM method



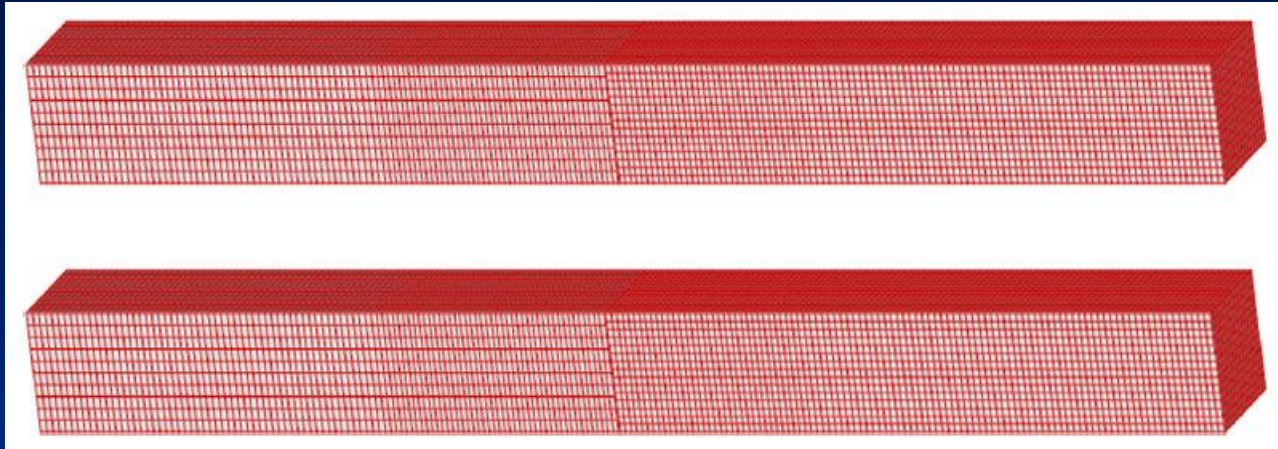
## Results of the DLM method

- **Test 3** A block of aluminum colliding with a resting block of 304 stainless steel

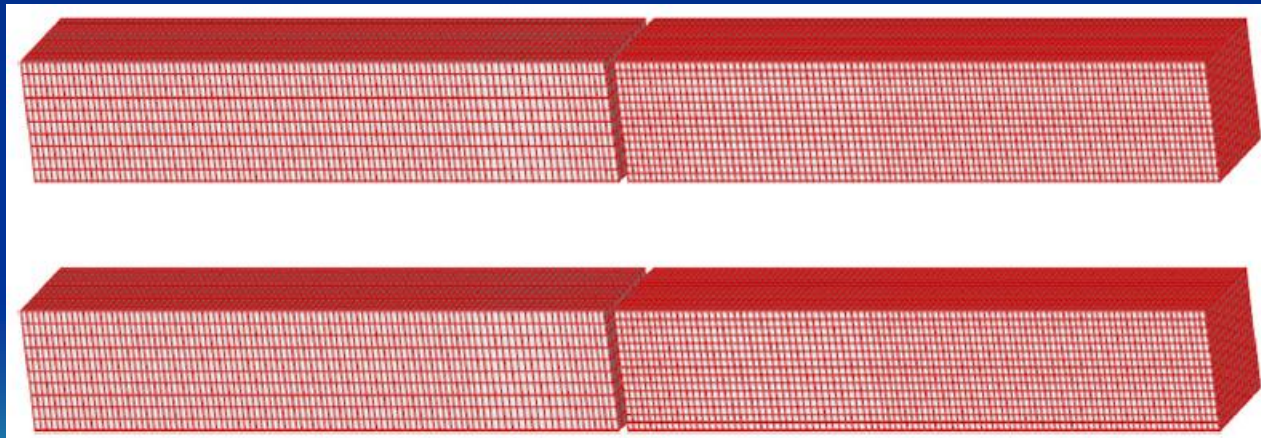


The initial meshes

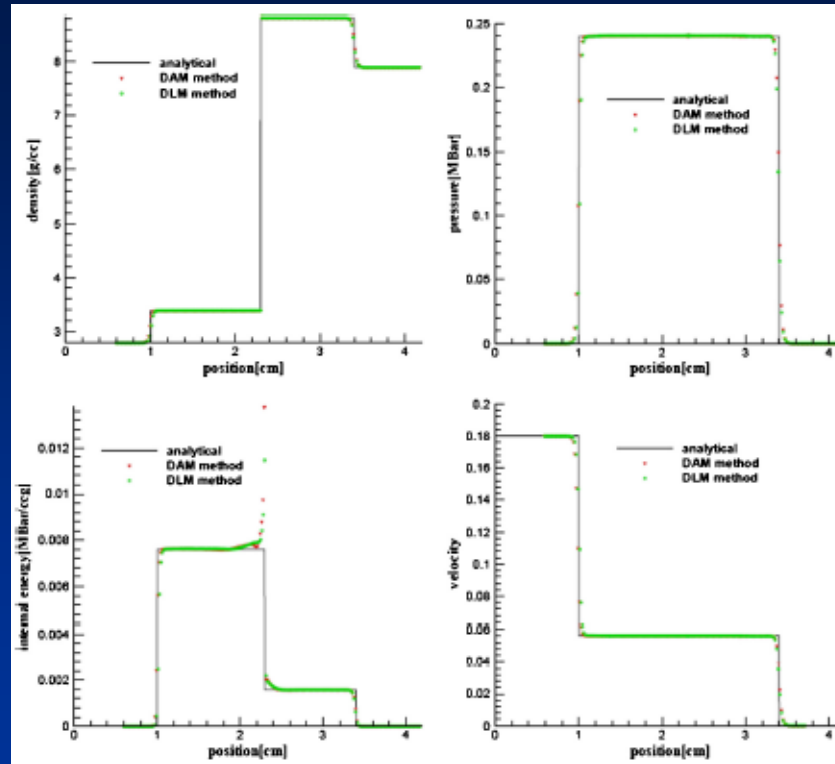




The mesh at  $t=2.25\mu\text{s}$  calculated by the DAM method (top) and the mesh at  $t=2.25\mu\text{s}$  calculated by the DLM method (bottom).



The mesh at  $t=8.25\mu\text{s}$  calculated by the DAM method (top) and the mesh at  $t=2.25\mu\text{s}$  calculated by the DLM method (bottom).



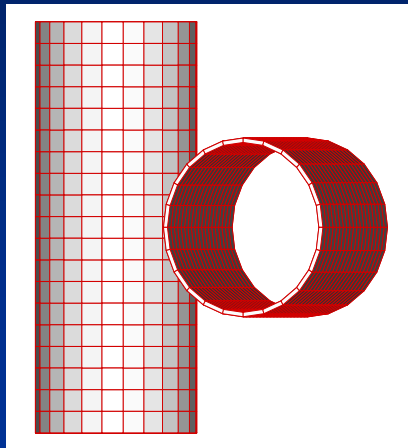
The density (top-left), pressure (top-right), internal energy (bottom-left) and velocity (bottom-right) at  $t=3.25\mu\text{s}$  calculated by the DAM method and the DLM method.

- **Test 4** Contact–impact between two tubes with the same stiffness

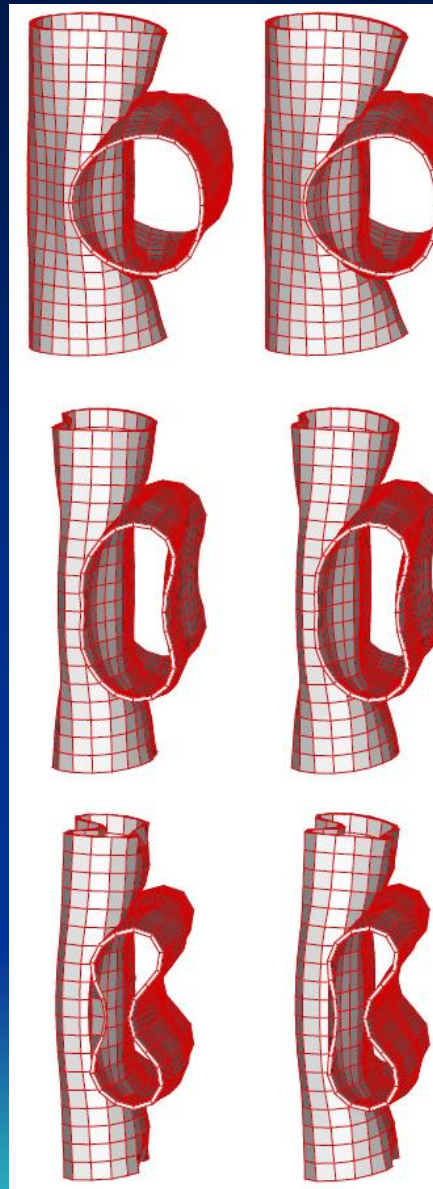
The calculation results are shown in the animation.







The initial meshes



*2ms*

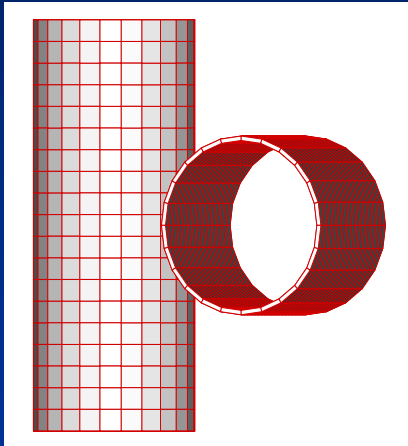
*4ms*

*6ms*

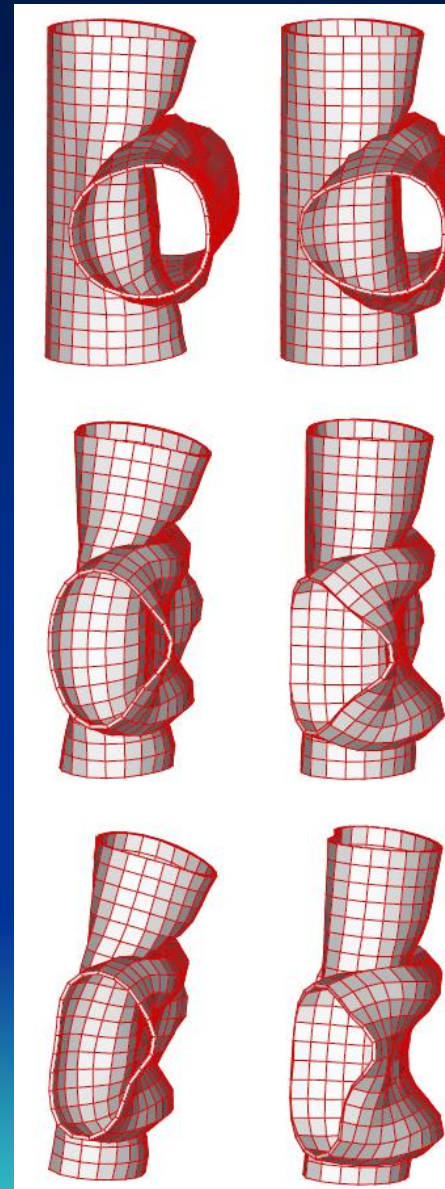
- **Test 5** Contact–impact between two tubes with different stiffness

The calculation results are shown in the animation.





The initial meshes



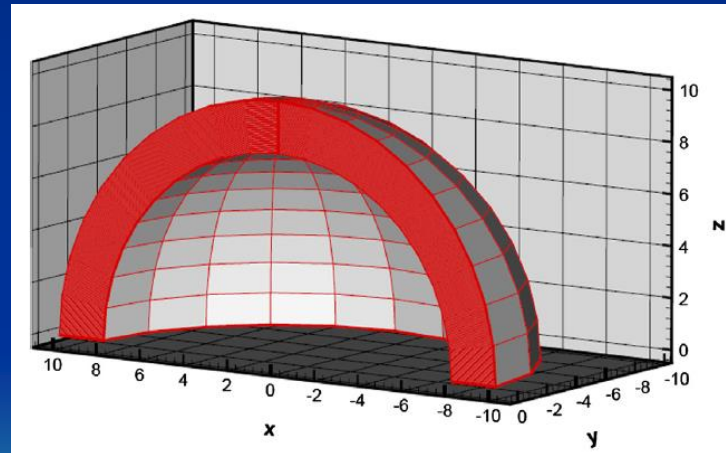
*1ms*

*2ms*

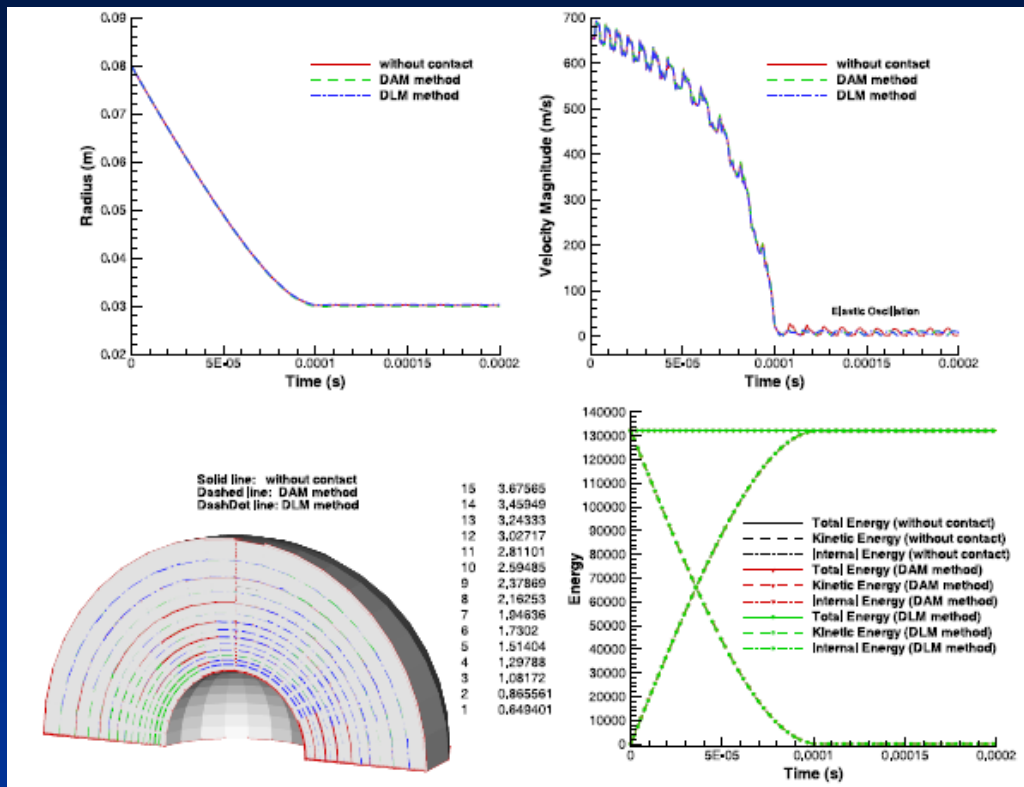
*3ms*

- **Test 6** Incompressible plastic collapse of spherical beryllium shell

The inner and outer radius of the shell are set at  $8cm$  and  $10cm$  respectively. The initial material density and pressure are uniform and constant. The initial radial velocity, however, is not uniform: it is given by the relation  $U(r) = -U_0 (R_i/r)^2$

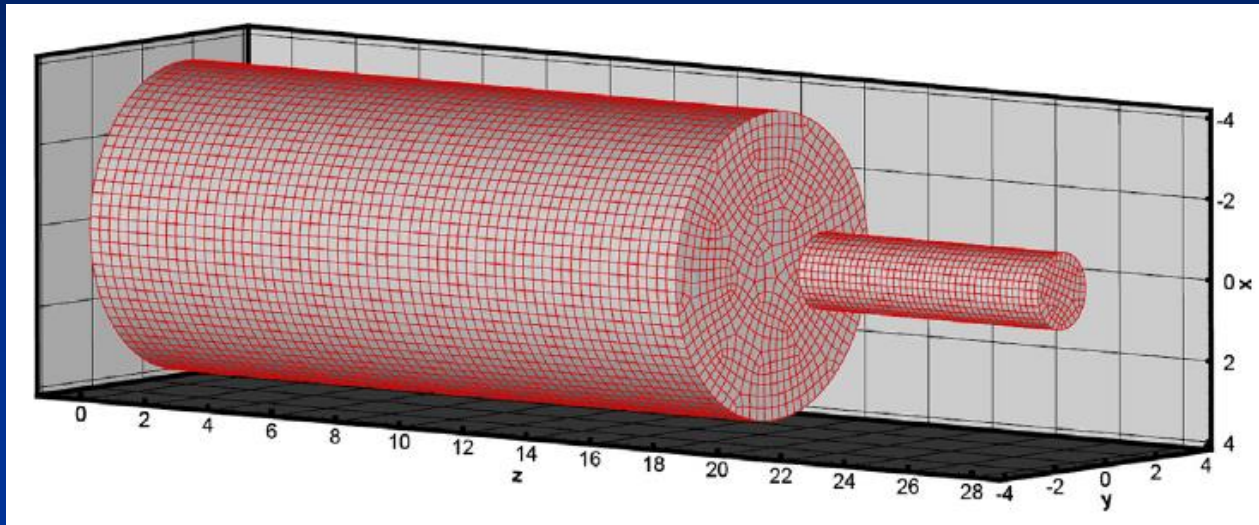


The initial meshes



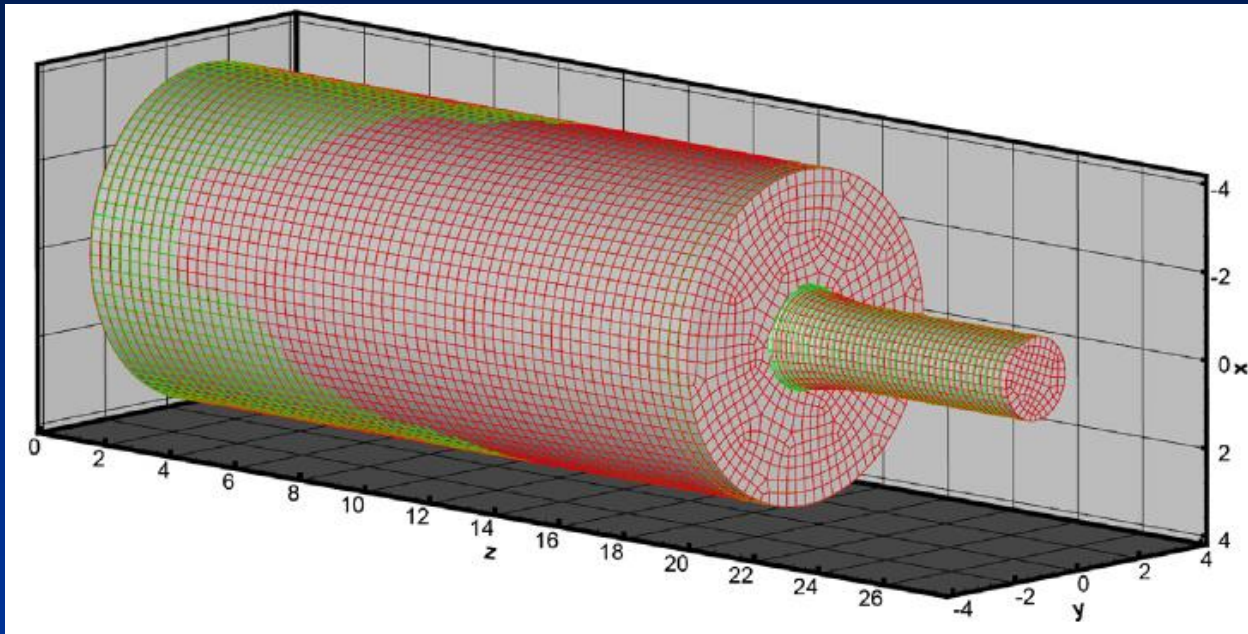
Locus of inner radius (top-left), history of velocity magnitude (top-right), contours of effective plastic strain at  $t=100.0\mu\text{s}$  (bottom-left), and history of energy conversion (bottom-right) obtained by computation without a contact surface and computation with the DAM method and the DLM method.

- **Test 7** Taylor–Anvil experiments

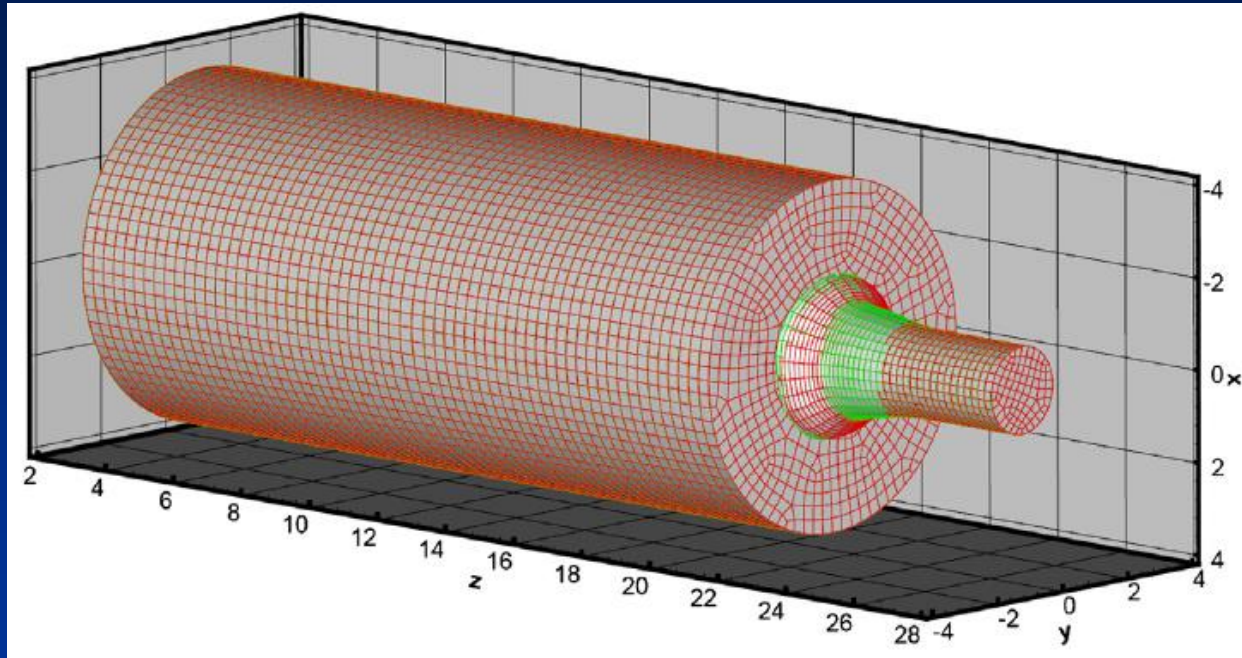


**The initial meshes**





The meshes at the time of  $149.0\mu\text{s}$  after the collision calculated by the DAM method and the DLM method for the case that the initial velocity is  $0.0083\text{ cm}/\mu\text{s}$ .



The meshes at the time of  $149.0\mu\text{s}$  after the collision calculated by the DAM method and the DLM method for the case that the initial velocity is  $0.0205\text{ cm}/\mu\text{s}$ .



## The results of Taylor experiments

Velocity cm/ $\mu$ s	Initial diameter	Initial length	Final diameter	Final length
0.0083	1.91	7.51	2.36	7.03
0.0205	1.89	7.50	3.66	5.45

Results obtained by computation with the DAM method.

Velocity cm/ $\mu$ s	Final diameter	Final length	Diameter error	Length Error
0.0083	2.346	7.093	-0.014	0.063
0.0205	3.474	5.571	-0.186	0.121

Results obtained by computation with the DLM method.

Velocity cm/ $\mu$ s	Final diameter	Final length	Diameter error	Length error
0.0083	2.390	7.084	0.030	0.054
0.0205	3.510	5.564	-0.150	0.114

# 7. Conclusion

- **Two new three-dimensional contact algorithms for staggered Lagrangian Hydrodynamics are presented. They are named the discrete accurate matching method and the discrete Lagrangian multiplier method.**
- **A series of standards and application examples show that both methods are robust and have high computational accuracy. Both methods can handle self contact.**



**Thanks for your attention!**

